ACS OMEGA

http://pubs.acs.org/journal/acsodf

Article

Phthalides Isolated from the Endolichenic *Arthrinium* sp. EL000127 Exhibits Antiangiogenic Activity

Chathurika D. B. Gamage,[‖] Kyungha Lee,[‖] So-Yeon Park, Mücahit Varlı, Chang Wook Lee, Seong-Min Kim, Rui Zhou, Sultan Pulat, Yi Yang, İsa Taş, Jae-Seoun Hur, Kyo Bin Kang,* and Hangun Kim*

Cite This: *ACS Omega* 2023, 8, 12548−12557

Read Online

ACCESS | Metrics & More | Article Recommendations | Supporting Information

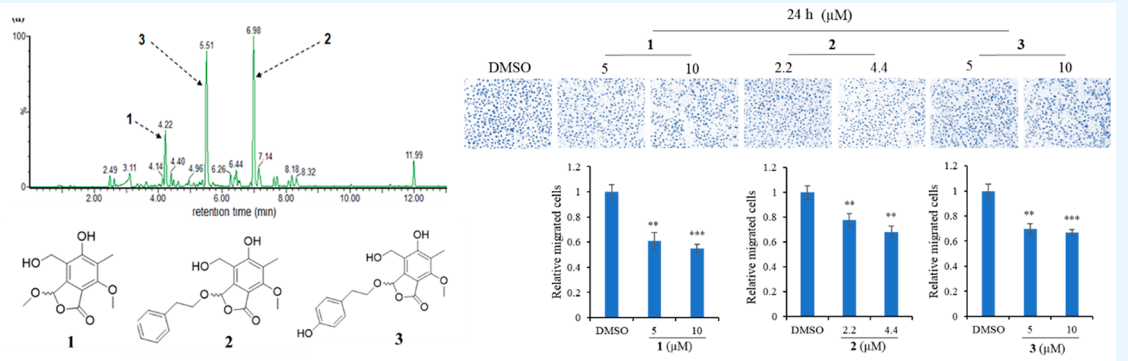

ABSTRACT: Endolichenic fungi (ELF) produce specialized metabolites that have various medicinal properties. Inhibition of tumor angiogenesis efficaciously suppresses many types of cancer. This study aimed to discover novel antiangiogenic agents from specialized metabolite extracts of ELF strains isolated from Korean lichens. The EtOAc extracts of 51 ELF strains were subjected to a screening pipeline consisting of cell viability, scratch wound healing, and Transwell migration assays. The EtOAc extract of *Arthrinium* sp. EL000127 showed the most potent inhibitory activity against the chemotactic migration of human umbilical vein endothelial cells (HUVEC). Targeted isolation on the major LC-MS peaks exhibited a previously known phthalide, 3-*O*-methylcyclopolic acid (**1**), and two unknown analogues of **1**, 3-*O*-phenylethylcyclopolic acid (**2**) and 3-*O*-*p*-hydroxyphenylethylcyclopolic acid (**3**). The structures were characterized by MS and NMR analyses. All the isolates were acquired and applied to bioassays as racemates due to spontaneous racemization. Among the isolates, compound **3** effectively inhibits HUVEC motility by suppressing mRNA expressions of genes regulating epithelial cell survival and motility, which suggested that compound **3** is a potent antiangiogenic agent suitable for further exploration as a potential novel therapeutic against cancers.

Lichens are a symbiont between a fungus (the mycobiont) and a cyanobacterium or a green alga (the hotobiont); lichens rarely contain both a cyanobacterium and a green alga.[1] Lichen thalli are comprised of an unknown number of organisms, and endolichenic microbes reside inside lichen thalli without producing any visible disease symptoms.[2] There are two main types of endolichenic microbes: endolichenic fungi (ELF) and endolichenic bacteria. Oligotrophic endolichenic fungi do not damage or support the production of fructifications at the thallus surface.[3] Some ELF species produce bioactive specialized metabolites that have medicinal and economic potential. Examples of the chemically diverse array of bioactive specialized metabolites include alkaloids, steroids, xanthones, benzopyranoids, peptides, and allycylic compounds. These metabolites have cytotoxic, antioxidant, antifungal, and antibacterial bioactivities, which are very important qualities in drug development in the pharmaceutical industry.[4,5] The ability of ELF to produce unique specialized metabolites with anticancer properties provides a novel approach for identifying effective cancer therapeutics.

Two cellular processes, vasculogenesis and angiogenesis, are involved in the development of the vasculature during embryogenesis. The development of new endothelial cells and their assembly into tubes is called vasculogenesis, and the growth of blood vessels from the existing vasculature is called angiogenesis.[6] After this morphogenesis, the normal vasculature becomes silent in the adult body, except during wound healing and female reproductive cycling.[7] By contrast,

Received: February 10, 2023
Accepted: March 14, 2023
Published: March 21, 2023

https://doi.org/10.1021/acsomega.3c00876
ACS Omega 2023, 8, 12548−12557

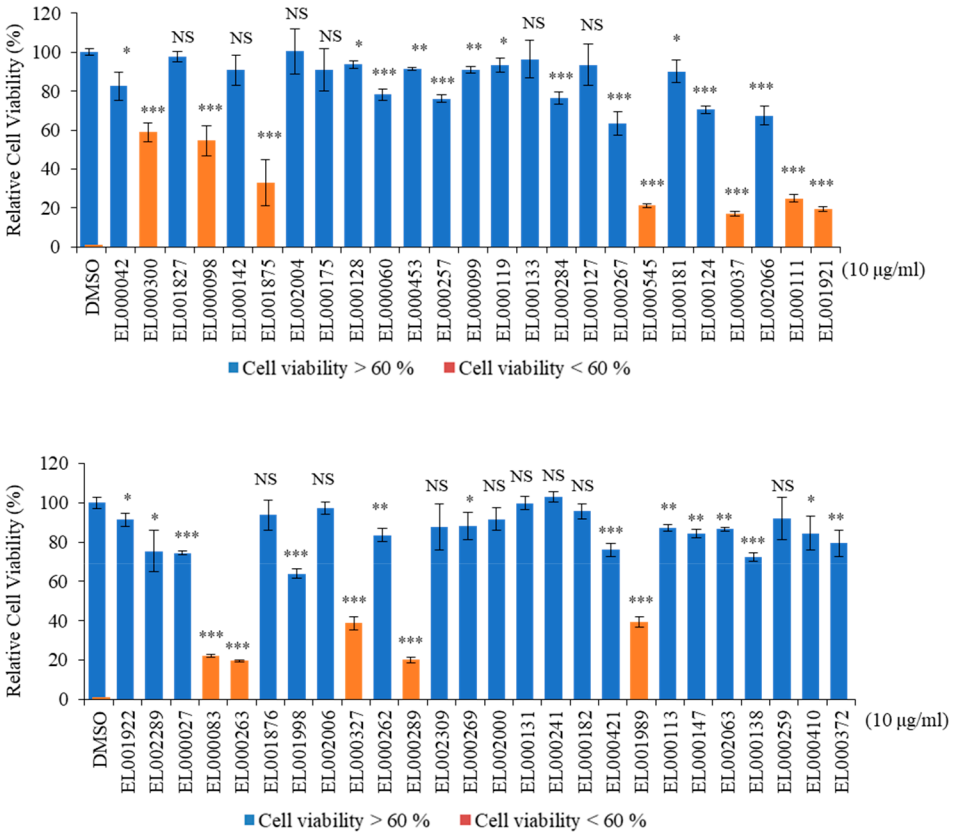

Figure 1. Cytotoxic effects of 51 ELF extracts isolated from Korean Lichens on HUVEC. HUVEC were treated with 51 ELF extracts at 10 μg/mL for 48 h, and cell viability was measured by MTT assay. Data are represented as mean ± SD (standard deviation), $n = 3$. *$p < 0.05$; **$p < 0.01$; ***$p < 0.001$; NS, no significant difference when compared with the DMSO-treated group in each cell line.

angiogenesis is constantly activated during cancer tumorigenesis to support tumor progression by forming new blood vessels to maintain a continuous supply of oxygen and nutrients.[8] Therefore, suppressing angiogenesis is one of the strategies of cancer therapeutics. The development of new chemical agents that inhibit angiogenesis is required to suppress tumor invasion and metastasis and eventually to inhibit cancer development.

There is a long history of investigating lichen-derived substances for pharmaceutical properties, especially for their use as anticancer agents.[9−11] The investigation of the pharmacological properties of the specialized metabolites of ELF for medicinal purposes is a fast-growing area of research. But there are no studies investigating the ability of ELF-derived compounds to inhibit cancer by inhibiting tumor angiogenesis. Therefore, this study aimed to screen out potential antiangiogenic agents from specialized metabolites biosynthesized by ELF isolated from our collection of Korean lichens. Our findings revealed that 3-*O*-*p*-hydroxyphenylethylcyclopolic acid (**3**) derives from *Arthrinium* sp. EL000127 inhibited angiogenesis by suppressing HUVEC survival and motility.

RESULTS AND DISCUSSION

The cytotoxic effect of the 51 ELF extracts (Table S1) on HUVEC was assessed by MTT assay. As shown in Figure 1, HUVEC had varying cell viabilities when treated with the ELF extracts at a concentration of 10 μg/mL. Among the 51 ELF extracts tested, 39 exhibited low or no cytotoxicity on HUVEC (cell viability >60%) and were subjected to the further step for evaluating the ability to inhibit angiogenesis. Cell migration plays a very important role in angiogenesis as it is the pivotal step for the formation of blood vessels by endothelial cells.[12] To identify the inhibitory ability of the 39 ELF extracts against HUVEC migration, the wound healing assay was performed. 33 ELF extracts showed measurable effect on HUVEC migration (Figures 2a and S1). The results revealed that ten ELF extracts (RWD < 100%), from strains EL002004, EL000175, EL000257, EL000099, EL000127, EL000181, EL001922, EL000027, EL001876, and EL001998, caused a lower relative wound density (RWD) in HUVEC than the control at 10 μg/mL (Figure 2b). The ten extracts were subjected to a Transwell migration assay, to evaluate the inhibitory effect of the ELF extracts on the chemotactic motility of HUVEC. EL000127 showed the highest inhibitory effect (40%) against the chemotactic motility of HUVEC (Figure 3a,b). As EL000127 was the most promising candidate among the tested strains, it was subjected to further chemical and biological characterization. Angiogenesis is initiated by vessel sprouting, which is mainly driven by VEGF signaling.[13] Therefore, suppressing endothelial cell migration in response to a signal stimulus is a key step in inhibiting tumor angiogenesis. In our screening, the extract of *Arthrinium* sp. EL000127 showed the more potent suppression of HUVEC migration in the presence of VEGF than any other candidates; it also suppressed mechanotaxic migration of HUVEC in the wound healing assay.

EL000127 was an ELF strain isolated from a lichen thallus of *Cladonia squamosal* collected from Mt. Halla, Jeju Island, in 2009. According to ITS sequence analysis based on BLAST searches of the GenBank database (GenBank Accession No.

https://doi.org/10.1021/acsomega.3c00876
ACS Omega 2023, 8, 12548−12557

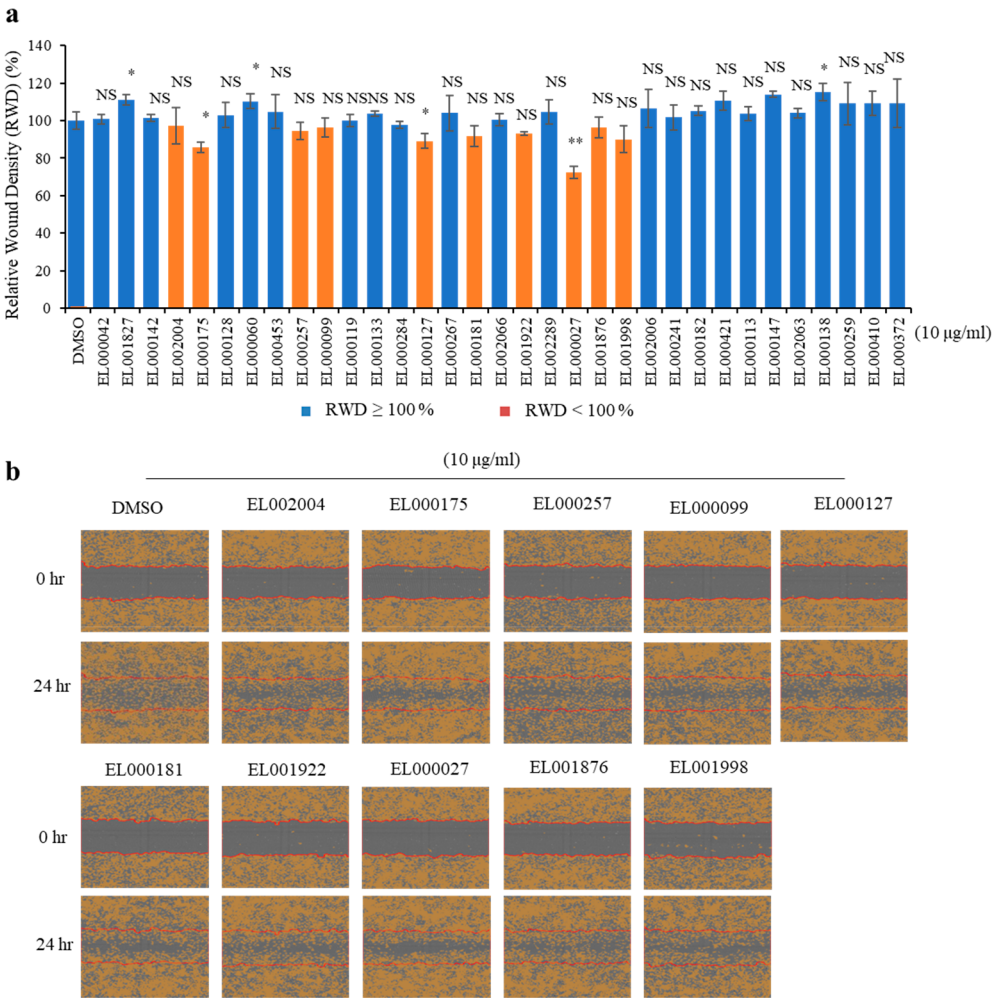

Figure 2. Ten ELF extracts inhibited HUVEC migration in the wound healing assay. (a) Quantitative analysis of the migratory ability of HUVEC expressed as the density of the wound region relative to the density of the cell region (RWD) after the treatment with the extracts (10 μg/mL) of 33 ELF. Three images per well were acquired, and scanning was performed every 2 h for 24 h. (b) EL002004, EL000175, EL000257, EL000099, EL000127, EL000181, EL001922, EL000027, EL001876, and EL001998 (10 μg/mL) inhibited HUVEC migration in the wound healing assay. Data represent mean ± SD (standard deviation), $n = 3$. *$p < 0.05$; **$p < 0.01$; NS, no significant difference compared with the DMSO-treated group.

MW629845), EL000127 showed 98.65% similarity to the fungus *Arthrinium pseudosinense*, which suggested EL000127 is a member of the genus *Arthrinium*. Species of *Arthrinium pseudosinense* belong to the family *Apiosporaceae* of the genus *Arthrinium* Kunze. Endophytes, pathogens, and saprobes isolated from various substrates such as lichens, plants, soil debris, and marine algae belong to the genus *Arthrinium* Kunze.[14,15] To the best of our knowledge, this is the first study to reveal the promising bioactivity of specialized metabolites of ELF in lichen *Cladonia squamosa*.

LC-MS/MS analysis on the *Arthrinium* sp. EL000127 extract exhibited several chromatographic peaks. Putative identification was tried using reference spectral library matching which is a part of a molecular networking workflow in GNPS;[16] however, none of the spectra were annotated. Three chromatographic peaks showing high ion intensities in the LC-MS base peak ion (BPI) chromatogram were prioritized and isolated to afford compounds **1**−**3** (Figure 4a,b).

Compound **1**, of which the molecular formula was $C_{12}H_{14}O_6$ (HRESIMS m/z 253.0723 $[M - H]^-$, calcd for $C_{12}H_{13}O_6$, 253.0712), was identified as 3-*O*-methyl-cyclopolic acid by comparing the MS and NMR spectra with those in ref 17. The ^{1}H and ^{13}C NMR data of **2** contained signals similar to those of **1**, but NMR signals of a phenyl group [δ_H 7.32 (3H, m) and 7.22 (2H, m)], a methylene group [δ_C 36.1/δ_H 2.94 (2H, m), C/H-7′], and an oxygenated methylene group [δ_C 70.4/δ_H 3.90 (1H, m) and 4.08 (1H, dt, J = 9.3, 6.0 Hz), C/H-8′] suggested an additional presence of a phenylethyl moiety. The ^{1}H−^{1}H COSY correlations between H-7′ and H-8′ and the HMBC correlations from H-2′/5′ (δ_H 7.32) to C-7′ confirmed the spin system of the phenylethyl group, and the HMBC from H-3 (δ_H 6.02) to C-8′ confirmed its attachment at C-3 via an ether bond (Figure 4c). The molecular formula of **2**, which was suggested as $C_{19}H_{20}O_6$ by its HRESIMS m/z 343.1186 $[M - H]^-$ (calcd for $C_{19}H_{19}O_6$, 343.1182), supported the structural characterization by NMR. Consequently, compound **2** was determined to be 3-*O*-phenylethyl-cyclopolic acid. The molecular formula of compound **3** was determined as $C_{19}H_{20}O_7$ based on its HRESIMS deprotonated molecular ion peak at m/z 359.1136 $[M - H]^-$ (calcd for $C_{19}H_{19}O_7$, 359.1131). The molecular formula suggested that compound **3** is a monooxygenated analogue of **2**. The ^{1}H NMR spectrum of **3** exhibited an A_2B_2 aromatic spin system [δ_H 7.06 (2H, d, J =

https://doi.org/10.1021/acsomega.3c00876
ACS Omega 2023, 8, 12548−12557

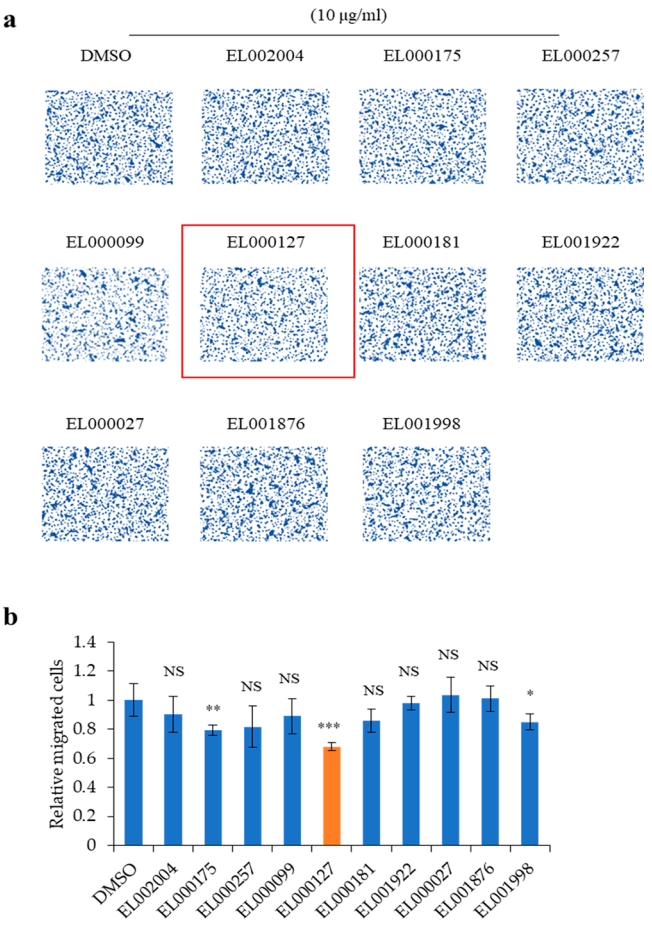

Figure 3. EL000127 was the most effective inhibitor of the chemotactic motility of HUVEC in a Transwell migration assay. (a) Transwell migration assays of HUVEC under chemotactic VEGF stimulation treated with extracts of EL002004, EL000175, EL000257, EL000099, EL000127, EL000181, EL001922, EL000027, EL001876, and EL001998 (10 μg/mL). (b) Quantitative analysis of the relative migration of HUVEC (under chemotactic VEGF stimulation) after treatment with ELF extracts. Representative images are shown from three independent experiments. Data represent mean ± SD (standard deviation), n = 3. $^{**}p < 0.01$; $^{***}p < 0.001$; NS, no significant difference when compared with the DMSO-treated group.

8.5 Hz) and 6.72 (2H, d, J = 8.5 Hz)], which indicated the presence of a *p*-hydroxyphenylethyl group in **3**. Thus, compound **3** was identified as 3-*O*-*p*-hydroxyphenylethyl-cyclopolic acid.

Compounds **1**−**3** showed no optical activity in polarimeter and ECD analysis, which indicated that all the isolates are racemic mixtures. Compound **1** was previously reported to show spontaneous racemization of the phthalide scaffold,[17] and similar phenomena were reported on other phthalides.[18−20] Our attempt on the chiral separation of compound **3** confirmed the equal amounts of enantiomers (Figure 4d); however, they could not be kept in enantiomerically pure form due to the fast rate of racemization. Thus, all the isolates were subjected to bioassays as racemic mixtures. Based on the previously suggested mechanisms of phthalide racemization via aldehyde−carboxylic acid tautomers,[19,20] compounds **1**−**3** were proposed to racemize via their enol ether tautomers (Figure 4e).

The cell viability of HUVEC was measured by MTT assay after treatment with various concentrations of compounds **1**−**3** for 48 h. Cell viability was dose-dependently decreased by treatments (Figure 5). Compounds **1**−**3** exhibited very weak cytotoxicity against HUVEC with IC_{50} values of 215.6 μM, 43.8 μM, and 1.83 mM, respectively. Nontoxic concentrations of **1**−**3** were used for further investigations on angiogenesis. To determine the effect of the isolates on the chemotactic motility of HUVEC induced by VEGF, Transwell migration assay was performed (Figure 6a).

Compounds **1** and **3** inhibited chemotactic motilities of HUVEC by approximately 40% and 30% at 5 μM and 45% and 33% at 10 μM after 24 h, respectively, while **2** inhibited them by approximately 22% and 32% at 2.2 and 4.4 μM, respectively (Figure 6b). mRNA expressions of genes regulating endothelial cell survival and motility were tested after the treatment with **1** and **3** at the concentration of 10 μM and **2** at the concentration of 4.4 μM for 24 h. Compound **3** significantly decreased the expressions of VEGF and some genes related to epithelial cell survival, Akt and mTOR. Furthermore, **3** significantly downregulated the expressions of Src, cdc42, and MAPK genes that regulate the migration of epithelial cells. Compound **2** significantly decreased the expressions of mTOR, Src, cdc42, and MAPK and **1** significantly decreased the mRNA levels of mTOR and Src (Figure 6c). In addition, **3** significantly suppressed the phosphorylation of Akt and mTOR as detected by Western blotting (Figure S2). VEGF is the pivotal factor of angiogenesis. Upon the binding of VEGF to VEGFR, phosphorylated VEGFR activates downstream signaling and initiates angiogenesis by recruiting endothelial progenitor from the bone marrow and promoting HUVEC proliferation.[21] Phosphorylation of Akt via VEGF signaling induces the phosphorylation of mTOR and eventually promotes HUVEC proliferation.[22] Activation of the PI3K/Akt/mTOR signaling pathway plays a key role in regulating angiogenic functions in both epithelial and tumor cells. While regulating many cellular functions in endothelial cells such as survival, migration, proliferation, and blood vessel formation, PI3K/Akt/mTOR signaling promotes angiogenesis by stimulating the secretion of VEGF and modulating the expressions of nitric oxide and angiopoietin in tumor cells. Furthermore, activation of mTOR in tumor cells induces HIF-1α mediated VEGF production under hypoxia.[23,24] Cdc42 is a small GTP-binding protein which belongs to the Rho family of GTPases. Cdc42 regulates endothelial cell motility by controlling the movements of actin cytoskeleton, Rac-dependent formation of lamellipodia, and maintaining cell polarity. Activation of Src by VEGFR2 led to the activation of RhoA which plays a significant role in endothelial cell migration via causing stress fiber formation[25] (Figure 6d). Taken together, compound **3** effectively suppresses angiogenesis at a 24 h time point by significantly decreasing HUVEC survival and migration. As both compounds **1** and **2** significantly suppressed the chemotactic motility of HUVEC, further investigations are required in different time points to confirm their antiangiogenic effects.

Our study demonstrates that specialized metabolites of endolichenic fungi are a promising source for discovering anticancer agents and highlights the urgent need for and importance of thorough investigations into the bioactive metabolites of ELF.

EXPERIMENTAL SECTION

Isolation and Culture of the Endolichenic Fungal Strains. Lichen specimens collected mainly from different

https://doi.org/10.1021/acsomega.3c00876
ACS Omega 2023, 8, 12548−12557

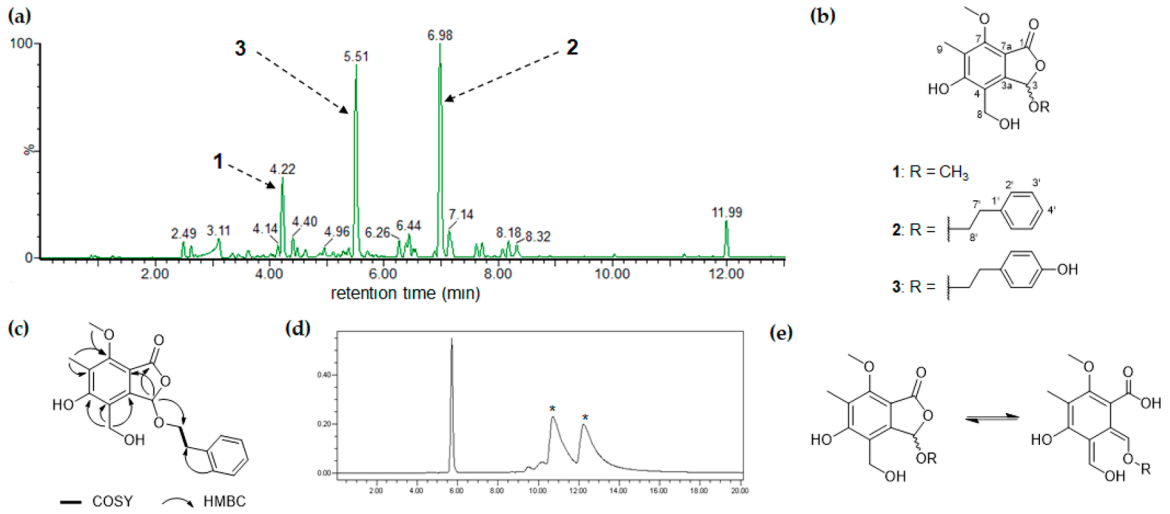

Figure 4. Isolation and structural identification of compounds **1**−**3** from *Arthrinium* sp. EL000127. (a) The LC-MS base peak ion (BPI) chromatogram of the *Arthrinium* sp. EL000127 extract. Isolated compounds are denoted on the corresponding chromatographic peaks. (b) Chemical structures of compounds **1**−**3**. (c) Key ^{1}H−^{1}H COSY and HMBC correlations of compound **2**. (d) The HPLC chromatogram (UV 280 nm) of the chiral separation of compound **3**. Two enantiomers of **3** are represented with asterisks. (e) Proposed scheme for spontaneous racemization of compounds **1**−**3**.

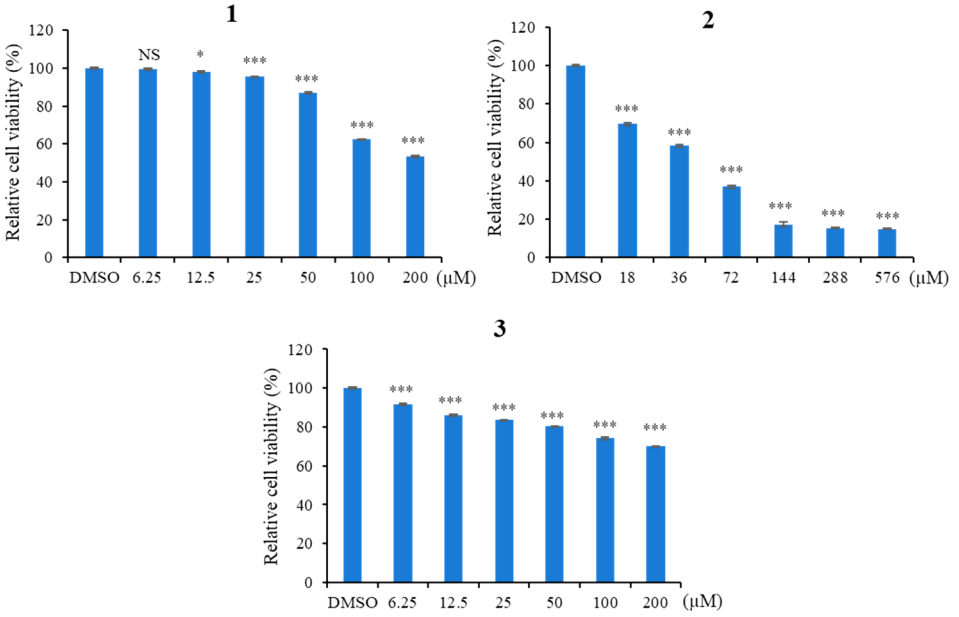

Figure 5. Compounds **1**−**3** decreased cell viability of HUVEC. HUVEC was treated with concentrations from 6.25 to 200 μM of compounds **1** and **3** and 18 to 576 μM of compound **2** for 48 h. Relative cell viability was measured by MTT assay. Data represent mean ± SD (standard deviation), n = 3. *p < 0.05; ***p < 0.001; NS, no significant difference when compared with the DMSO-treated group.

parts of Jeju Island and Mt. Jili in Jeollanamdo in South Korea during field trips from 2009 to 2010 were identified at the Korean Lichen Research Institute (KoLRI) at Sunchon National University, Korea. Lichen specimens of *Cladonia squamosal* collected from Mt. Halla in Jeju Island in 2009 were identified at KoLRI. Voucher specimens were deposited in KoLRI (https://cc.aris.re.kr/cc/app/main/mainView.do). Fifty-one endolichenic fungi associated with Korean lichens, including EL000127, were isolated using a surface sterilization method.[26] The isolated strains were maintained in potato dextrose agar (PDA) media at 25 °C. For screening and preparative scale cultures, ELF mycelia grown on agar were cut and inoculated into 200 mL of potato dextrose broth (PDB) in 500 mL Erlenmeyer flasks and incubated at 25 °C in a shaking incubator at 150 rpm for 3−4 weeks. The specialized metabolites were extracted by adding 200 mL of EtOAc into each flask, filtering, and separating the EtOAc-soluble layer. Crude extracts were evaporated to dryness under a vacuum using a rotary evaporator. The crude extracts were dissolved in 100% DMSO and were subjected to the screening.

Identification of *Arthrinium* sp. EL000127 by Internal Transcribed Spacer Sequencing. DNA was extracted from EL000127 cultured on PDA using a DNeasy Plant Mini Kit following the manufacturer's protocols (Qiagen, Hilden, Germany). The internal transcribed spacer (ITS) region of the rDNA was amplified with the universal primers ITS1F (5′-CTTGGTCATTTAGAGGAAGTAA-3′)[27] and LR5 (5′-ATC-CTGAGGGAAACTTC-3′),[28] as described by Yang et al.[29]

https://doi.org/10.1021/acsomega.3c00876
ACS Omega 2023, 8, 12548−12557

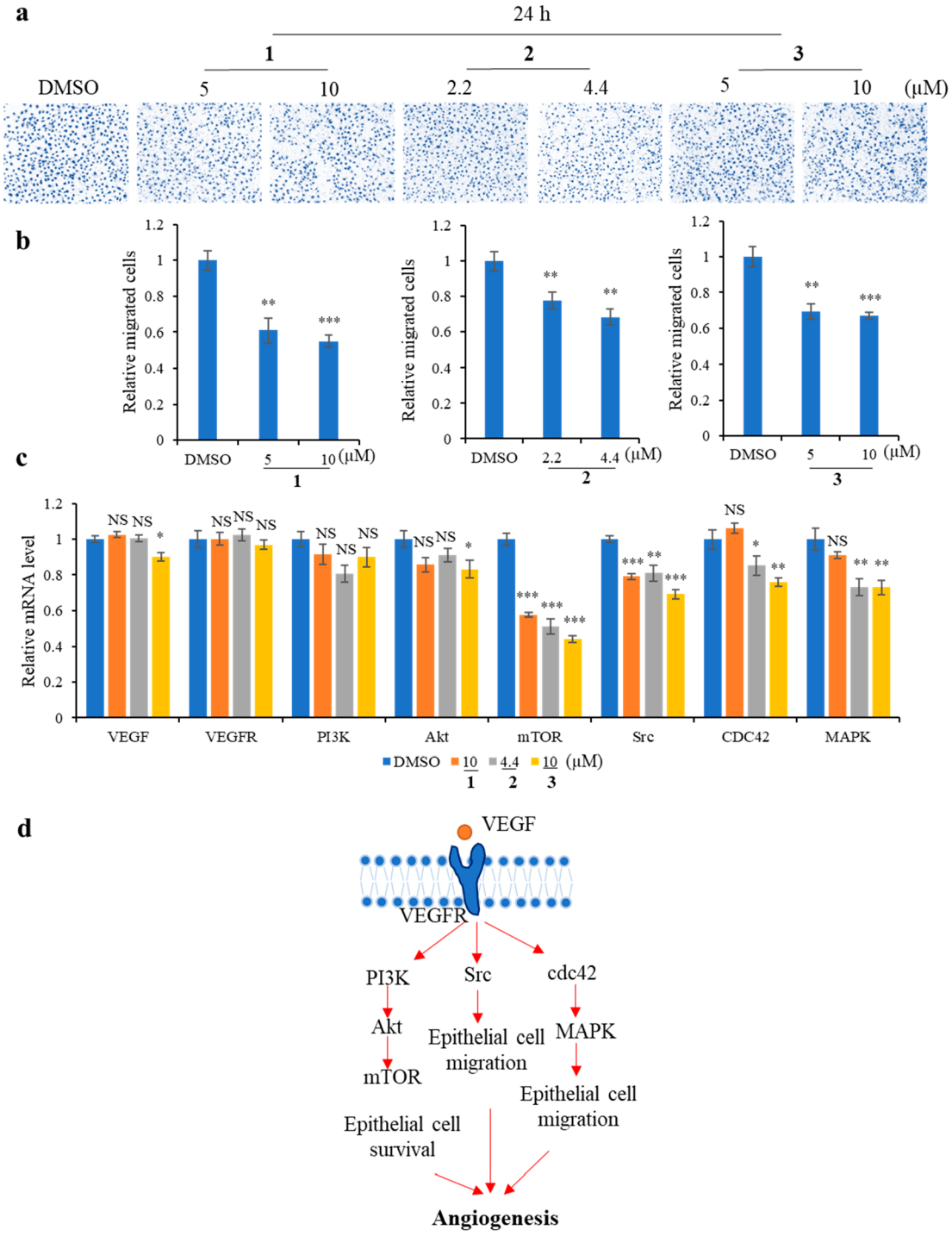

Figure 6. Compound **3** from EL000127 suppressed angiogenesis. (a) Images of migrated HUVEC induced by VEGF after the treatment with **1**, **2**, and **3** at the concentrations of 5 and 10 μM (**1** and **3**) and 2.2 and 4.4 μM (**2**) for 24 h (b) Quantitative analysis of migrated HUVEC against the treatment of **1**, **2**, and **3**. (c) Relative mRNA levels of genes regulating epithelial cell survival and migration after the treatment with **1**, **2**, and **3** at the concentrations of 10 μM (**1** and **3**) and 4.4 μM (**2**) for 24 h. Representative images are shown from three independent experiments. Data represent mean ± SD (standard deviation), $n = 3$. *$p < 0.05$; **$p < 0.01$; ***$p < 0.001$; NS, no significant difference when compared with the DMSO-treated group. (d) Simple schematic representation of the VEGF signaling pathway involved in angiogenesis.

LC-MS/MS Analysis of the *Arthrinium* sp. EL000127 Extract. Specialized metabolites of *Arthrinium* sp. EL000127 were analyzed on a Waters Acquity I-Class UHPLC system coupled to a Waters VION IMS QTOF mass spectrometer (Waters Co., Milford, MA, U.S.A.). Chromatographic separations were performed on a Waters Acquity BEH C18 column (100 × 2.1 mm, 1.7 μm), which was eluted by a mobile phase comprising of 0.1% formic acid in water (A) and MeCN (B). A stepwise gradient method at a constant flow rate (0.3 mL/min) was used with the following conditions: 10−100% of B (0−12 min), followed by 3 min of washing and 3 min of reconditioning. MS/MS analysis was performed in data-independent acquisition (MS^E) of negative ion mode. MS/MS spectral data matching was performed by the feature-based

https://doi.org/10.1021/acsomega.3c00876
ACS Omega 2023, 8, 12548−12557

Table 1. ^{1}H (500 MHz) and ^{13}C (125 MHz) NMR Spectroscopic Data of Compounds 1−3

	1[a]		2[b]		3[a]	
	δ_C	δ_H (J in Hz)	δ_C	δ_H (J in Hz)	δ_C	δ_H (J in Hz)
1	167.3		166.9		168.8	
3	101.4	6.30, s	100.3	6.02, s	102.2	6.34, s
3a	117.0		115.3		118.3	
4	162.2		162.4		163.8	
5	142.3		141.9		144.5	
6	120.8		121.9		122.2	
7	157.1		157.5		158.5	
7a	108.4		108.9		109.6	
8	57.2	4.86, d (13.2), 4.79, d (13.2)	59.0	4.49, d (13.8), 4.45, d (13.8)	58.7	4.67, d (13.4), 4.59, d (13.4)
9	7.4	2.15, s	8.7	2.11, s	8.5	2.14, s
3-OCH_3	55.0	3.54, s				
7-OCH_3	61.1	3.97, s	62.5	3.97, s	62.5	3.96, s
1′			138.5		130.5	
2′/5′			128.8	7.32, m	131.0	7.06, d (8.5)
3′/6′			129.3	7.22, m	116.2	6.72, d (8.5)
4′			126.9	7.32, m	157.0	
7′			36.1	2.94, m	36.2	2.86, t-like
8′			70.4	4.08, dt (9.3, 6.0), 3.90, m	71.8	3.98, dd (9.4, 6.6), 3.90, m

[a]In CD_3OD. [b]In $CDCl_3$.

molecular networking workflow in GNPS,[30] after the preprocessing using MS-DIAL.[31]

Isolation and Structural Elucidation of Compounds 1−3. The EtOAc extract of *Arthrinium* sp. EL000127 (3.2 g) was fractionated into seven fractions (E1−E7) by a preparative HPLC (Waters 600 system) equipped with a Hector C_{18} column (250 × 21.2 mm, 5 μm, RS Tech, Daejeon, Korea; eluted with 12 mL/min of H_2O-MeCN 90:10 → 10:90). Compound **2** (21.4 mg) was obtained from E7 (t_R 23.3 min) without any further purification due to the high purity. Compound **1** (5.7 mg, t_R 13.0 min) was obatined from E2 using a preparative HPLC with Hector C_{18} column (250 × 10 mm, 5 μm; eluted with 4 mL/min of H_2O-MeCN 70:30 → 55:45 for 0−30 min). E6 (52.3 mg) was further purified into compound **3** (3.3 mg, t_R 23.0 min) using a preparative HPLC with Hector C_{18} column (250 × 10 mm, 5 μm; eluted with 4 mL/min of isocratic 45% MeCN in H_2O). The chiral sepration of racemic **3** was performed with a CHIRAL IB column (250 × 10 mm, 5 μm, Daicel Chemical Industries, Ltd., Osaka, Japan) eluted with a mixture of *n*-hexane and EtOH (75:25, 4 mL/min). Two enantiomers showed chromatographic peaks at t_R 10.5 and 12.0 min, respectively. The optical rotations were obtained using a Jasco P-2000 polarimeter (Jasco, Tokyo, Japan) and electronic circular dichroism (ECD) was conducted with a Chirascan CD spectrometer (Applied Photophysics, Surrey, U.K.). NMR experiments were performed on a Bruker Avance III HD 500 MHz (Bruker, Billerica, MA, USA).

3-*O*-methyl-cyclopolic acid (**1**): light yellow amorphous powder; ^{1}H NMR and ^{13}C NMR data, see Table 1; HRESIMS m/z 253.0723 $[M - H]^-$ (calcd for $C_{12}H_{13}O_6$, 253.0712); the MS/MS spectrum is deposited in the GNPS spectral library, https://gnps.ucsd.edu/ProteoSAFe/gnpslibraryspectrum.jsp?SpectrumID=CCMSLIB00010128698#%7B%7D.[32]

3-*O*-phenylethyl-cyclopolic acid (**2**): yellow amorphous powder; ^{1}H NMR and ^{13}C NMR data, see Table 1; HRESIMS m/z 343.1186 $[M - H]^-$ (calcd for $C_{19}H_{19}O_6$, 343.1182); the MS/MS spectrum is deposited in the GNPS spectral library, https://gnps.ucsd.edu/ProteoSAFe/gnpslibraryspectrum.jsp?SpectrumID=CCMSLIB00010128671#%7B%7D.[33]

3-*O*-*p*-hydroxyphenylethyl-cyclopolic acid (**3**): yellow amorphous powder; ^{1}H NMR and ^{13}C NMR data, see Table 1; HRESIMS m/z 359.1136 $[M - H]^-$ (calcd for $C_{19}H_{19}O_7$, 359.1131); the MS/MS spectrum is deposited in the GNPS spectral library, https://gnps.ucsd.edu/ProteoSAFe/gnpslibraryspectrum.jsp?SpectrumID=CCMSLIB00010128697#%7B%7D.[34]

Original NMR FIDs are available at 10.5281/zenodo.7375204.[35]

Cell Culture. Human umbilical vein endothelial cells (HUVEC) were cultured in endothelial cell medium (ECM) (Sciencell, Carlsbad, CA, U.S.A.) supplemented with 5% fetal bovine serum (FBS), 1% penicillin/streptomycin solution (P/S), and 1% endothelial cell growth supplement (ECGS). Cells were maintained in a 5% CO_2 humidified atmosphere at 37 °C. HUVEC were purchased from Lonza Bioscience (Walkersville, MD, U.S.A.).

Cell Viability Assay. The MTT (3-(4,5-dimethylthiazol-2-yl)-2,5-diphenyltetrazolium bromide; Sigma, St. Louis, MO, U.S.A.) assay was performed to measure the proliferation and viability of HUVEC cells. Cells were seeded at a density of 3 × 10^3 cells/well in 96-well plates, treated with 51 different ELF extracts or compounds **1**−**3** for 48 h, and then incubated in the MTT reagent for 4 h. The medium was aspirated, and 150 μL of DMSO was added to each well. The absorbance was measured at 540 nm using a microplate reader and analyzed with Gen 5 (2.03.1) software (BioTek, Winooski, VT, U.S.A.).

Wound Healing Assay. HUVEC were plated at a density of 2 × 10^4 cells/well on 96-well ImageLock tissue culture plates (Essen BioScience, Ann Arbor, MI, U.S.A.) and grown overnight to confluence. Monolayer cells were scratched with a WoundMaker (Essen BioScience) to create precise and reproducible wounds in all wells. The cells were then washed twice with serum-free ECM to remove floating cells and incubated in ECM culture medium supplemented with 1% FBS. Cells were treated with 10 μg/mL of each of 39 ELF. Plates were imaged using an IncuCyte Zoom instrument with a

https://doi.org/10.1021/acsomega.3c00876
ACS Omega 2023, 8, 12548−12557

10× objective and analyzed using the standard scan type. Three images per well were acquired, and scanning was performed every 2 h for 24 h. The migration ability of HUVEC was expressed as the density of the wound region relative to the density of the cell region (relative wound density (RWD)) using IncuCyte Software. Three independent experiments were performed.

Transwell Migration Assay. The chemotactic motility of HUVEC was determined using a Transwell migration assay with an 8 μm pore size polycarbonate membrane Transwell (Corning, NY, U.S.A.) coated with 0.1% gelatin. Fresh ECM supplemented with 4 ng/mL vascular endothelial growth factor (VEGF; R&D Systems, Minneapolis, MN, U.S.A.) was placed in the lower chamber, and HUVEC (4×10^4 cells/well) were seeded in the top chamber. Then, cells were treated with 10 selected ELF extracts or compounds **1**−**3** for 24 h at 37 °C with 5% CO_2. After incubation, nonmigrated cells on the top surface of the membrane were gently scraped away with a cotton swab. The upper chambers were fixed and stained with a Diff-Quik kit (Sysmex, Kobe, Japan). The migrated cells were analyzed under a light microscope in five randomly selected fields. Each experiment was performed in triplicate.

Quantitative Real-Time PCR. Total RNA of HUVEC treated by compounds **1**−**3** for 24 h were extracted using RNAiso Plus (TaKaRa) according to the manufacturer's instructions. A total of 3 μg of RNA of each treated group were reverse transcribed to cDNA using M-MLV reverse transcriptase kit (Invitrogen, Carlsbad, CA, U.S.A.). mRNA expressions were measured using SYBR green reagent (Enzynomics, Seoul, South Korea), and analyses were performed by a CFX instrument (Bio-Rad, Hercules, CA, U.S.A.). The list of primers used are mentioned in Table S2.

Western Blotting. HUVEC were treated with 10 μM of **1** and **3** and 4.4 μM of **2** for 24 h, harvested, and lysed in lysis buffer. A total of 25 μg of proteins from each treatment group were separated by SDS-PAGE, transferred to a blotting membrane, and blocked by 5% skim milk for 1 h. Membranes were incubated with primary antibodies of Akt, p-Akt, mTOR, p-mTOR, and actin (Cell Signaling Technology, MA, U.S.A.) for 2 h at room temperature (RT) followed by the incubation with horseradish peroxidase-conjugated secondary antibodies (Thermo Fisher Scientific) for 1 h at RT. Protein bands were detected using chemiluminescence imaging (biomolecular imager, Amersham ImageQuant 800 Western blot imaging System) and measured by Multi Gauge 3.0. software. Relative density was calculated against the density of the actin bands.

Statistical Analysis. All experiments were performed in triplicates. Data were expressed as means ± standard deviation (SD). All statistical analyses were performed using IBM Statistical Package for Social Science (SPSS) version 22. The statistical significant between two groups was compared using the Student's t test. Unless indicated otherwise, a p-value < 0.05 was considered significant.

■ ASSOCIATED CONTENT

Supporting Information

The Supporting Information is available free of charge at https://pubs.acs.org/doi/10.1021/acsomega.3c00876.

Figure S1, effect of 33 ELF extracts on HUVEC migration in the IncuCyte wound healing assay; Figure S2, compound **3** significantly suppressed the phosphorylation of proangiogenic proteins in HUVEC; Table S1, fifty-one ELF isolated from Korean lichens were screened for their effects on cell viability; and Table S2, angiogenesis related primer list used in QRT-PCR (PDF)

■ AUTHOR INFORMATION

Corresponding Authors

Hangun Kim − *College of Pharmacy, Sunchon National University, Sunchon, Jeonnam 57922, Korea;* orcid.org/0000-0001-5889-8907; Phone: +82-61-750-3761; Email: hangunkim@sunchon.ac.kr

Kyo Bin Kang − *Research Institute of Pharmaceutical Sciences, College of Pharmacy, Sookmyung Women's University, Seoul 04310, Korea;* orcid.org/0000-0003-3290-1017; Phone: +82-2-2077-7103; Email: kbkang@sookmyung.ac.kr

Authors

Chathurika D. B. Gamage − *College of Pharmacy, Sunchon National University, Sunchon, Jeonnam 57922, Korea*

Kyungha Lee − *Research Institute of Pharmaceutical Sciences, College of Pharmacy, Sookmyung Women's University, Seoul 04310, Korea*

So-Yeon Park − *College of Pharmacy, Sunchon National University, Sunchon, Jeonnam 57922, Korea*

Mücahit Varlı − *College of Pharmacy, Sunchon National University, Sunchon, Jeonnam 57922, Korea*

Chang Wook Lee − *College of Pharmacy, Sunchon National University, Sunchon, Jeonnam 57922, Korea*

Seong-Min Kim − *College of Pharmacy, Sunchon National University, Sunchon, Jeonnam 57922, Korea*

Rui Zhou − *College of Pharmacy, Sunchon National University, Sunchon, Jeonnam 57922, Korea*

Sultan Pulat − *College of Pharmacy, Sunchon National University, Sunchon, Jeonnam 57922, Korea*

Yi Yang − *College of Pharmacy, Sunchon National University, Sunchon, Jeonnam 57922, Korea*

İsa Taş − *College of Pharmacy, Sunchon National University, Sunchon, Jeonnam 57922, Korea*

Jae-Seoun Hur − *Korean Lichen Research Institute, Sunchon National University, Sunchon, Jeonnam 57922, Korea*

Complete contact information is available at: https://pubs.acs.org/10.1021/acsomega.3c00876

Author Contributions

‖Chathurika D. B. Gamage and Kyungha Lee contributed equally.

Notes

The authors declare no competing financial interest.

■ ACKNOWLEDGMENTS

This work was supported by the National Research Foundation of Korea Grants NRF-2020R1C1C1007832, 2020R1C1C1004046, and 2022R1A5A2021216) funded by the Korea government (MSIP).

■ ABBREVIATIONS

CRC, colorectal cancer; ELF, endolichenic fungi; HUVEC, human umbilical vein endothelial cells

https://doi.org/10.1021/acsomega.3c00876
ACS Omega 2023, 8, 12548−12557

REFERENCES

(1) Aschenbrenner, I. A.; Cernava, T.; Berg, G.; Grube, M. Understanding Microbial Multi-Species Symbioses. *Frontiers in Microbiology*. **2016**, DOI: 10.3389/fmicb.2016.00180.

(2) Honegger, R.; Axe, L.; Edwards, D. Bacterial Epibionts and Endolichenic Actinobacteria and Fungi in the Lower Devonian Lichen Chlorolichenomycites Salopensis. *Fungal Biol.* **2013**, *117* (7), 512−518.

(3) Honegger, R. The Symbiotic Phenotype of Lichen-Forming Ascomycetes and Their Endo- and Epibionts BT. *Fungal Associations*; Springer: 2012; pp 287−339.

(4) Suryanarayanan, T. S.; Thirunavukkarasu, N. Endolichenic Fungi: The Lesser Known Fungal Associates of Lichens. *Mycology* **2017**, *8* (3), 189−196.

(5) Kellogg, J. J.; Raja, H. A. Endolichenic Fungi: A New Source of Rich Bioactive Secondary Metabolites on the Horizon. *Phytochemistry Reviews*; Springer: 2017; pp 271−293.

(6) Carmeliet, P.; Jain, R. K. Angiogenesis in Cancer and Other Diseases. *Nature* **2000**, *407* (6801), 249−257.

(7) Hanahan, D.; Weinberg, R. A. Hallmarks of Cancer: The next Generation. *Cell* **2011**, *144* (5), 646−674.

(8) Song, Y.; Dai, F.; Zhai, D.; Dong, Y.; Zhang, J.; Lu, B.; Luo, J.; Liu, M.; Yi, Z. Usnic Acid Inhibits Breast Tumor Angiogenesis and Growth by Suppressing VEGFR2-Mediated AKT and ERK1/2 Signaling Pathways. *Angiogenesis* **2012**, *15* (3), 421−432.

(9) Nguyen, T. T.; Yoon, S.; Yang, Y.; Lee, H. B.; Oh, S.; Jeong, M. H.; Kim, J. J.; Yee, S. T.; Crişan, F.; Moon, C.; Lee, K. Y.; Kim, K. K.; Hur, J. S.; Kim, H. Lichen Secondary Metabolites in Flavocetraria Cucullata Exhibit Anti-Cancer Effects on Human Cancer Cells through the Induction of Apoptosis and Suppression of Tumorigenic Potentials. *PLoS One* **2014**, *9* (10), e111575.

(10) Yang, Y.; Nguyen, T. T.; Jeong, M. H.; Crişan, F.; Yu, Y. H.; Ha, H. H.; Choi, K. H.; Jeong, H. G.; Jeong, T. C.; Lee, K. Y.; Kim, K. K.; Hur, J. S.; Kim, H. Inhibitory Activity of (+)-Usnic Acid against Non-Small Cell Lung Cancer Cell Motility. *PLoS One* **2016**, *11* (1), e0146575.

(11) Zhou, R.; Yang, Y.; Park, S.-Y.; Nguyen, T. T.; Seo, Y.-W.; Lee, K. H.; Lee, J. H.; Kim, K. K.; Hur, J.-S.; Kim, H. The Lichen Secondary Metabolite Atranorin Suppresses Lung Cancer Cell Motility and Tumorigenesis. *Sci. Rep.* **2017**, *7* (1), 8136.

(12) Staton, C. A.; Reed, M. W. R.; Brown, N. J. A Critical Analysis of Current in Vitro and in Vivo Angiogenesis Assays. *Int. J. Exp. Pathol.* **2009**, *90* (3), 195−221.

(13) Chappell, J. C.; Wiley, D. M.; Bautch, V. L. Regulation of Blood Vessel Sprouting. *Semin. Cell Dev. Biol.* **2011**, *22* (9), 1005−1011.

(14) Dai, D. Q.; Jiang, H. B.; Tang, L. Z.; Bhat, D. J. Two New Species of Arthrinium (Apiosporaceae, Xylariales) Associated with Bamboo from Yunnan, China. *Mycosphere* **2016**, *7* (9), 1332−1345.

(15) Senanayake, I. C.; Maharachchikumbura, S. S. N.; Hyde, K. D.; Bhat, J. D.; Jones, E. B. G.; McKenzie, E. H. C.; Dai, D. Q.; Daranagama, D. A.; Dayarathne, M. C.; Goonasekara, I. D.; Konta, S.; Li, W. J.; Shang, Q. J.; Stadler, M.; Wijayawardene, N. N.; Xiao, Y. P.; Norphanphoun, C.; Li, Q.; Liu, X. Z.; Bahkali, A. H.; Kang, J. C.; Wang, Y.; Wen, T. C.; Wendt, L.; Xu, J. C.; Camporesi, E. Towards Unraveling Relationships in Xylariomycetidae (Sordariomycetes). *Fungal Divers.* **2015**, *73* (1), 73−144.

(16) Wang, M.; Carver, J. J.; Phelan, V. V.; Sanchez, L. M.; Garg, N.; Peng, Y.; Nguyen, D. D.; Watrous, J.; Kapono, C. A.; Luzzatto-Knaan, T.; Porto, C.; Bouslimani, A.; Melnik, A. V.; Meehan, M. J.; Liu, W.-T.; Crüsemann, M.; Boudreau, P. D.; Esquenazi, E.; Sandoval-Calderón, M.; Kersten, R. D.; Pace, L. A.; Quinn, R. A.; Duncan, K. R.; Hsu, C.-C.; Floros, D. J.; Gavilan, R. G.; Kleigrewe, K.; Northen, T.; Dutton, R. J.; Parrot, D.; Carlson, E. E.; Aigle, B.; Michelsen, C. F.; Jelsbak, L.; Sohlenkamp, C.; Pevzner, P.; Edlund, A.; McLean, J.; Piel, J.; Murphy, B. T.; Gerwick, L.; Liaw, C.-C.; Yang, Y.-L.; Humpf, H.-U.; Maansson, M.; Keyzers, R. A.; Sims, A. C.; Johnson, A. R.; Sidebottom, A. M.; Sedio, B. E.; Klitgaard, A.; Larson, C. B.; Boya P, C. A.; Torres-Mendoza, D.; Gonzalez, D. J.; Silva, D. B.; Marques, L. M.; Demarque, D. P.; Pociute, E.; O'Neill, E. C.; Briand, E.; Helfrich, E. J. N.; Granatosky, E. A.; Glukhov, E.; Ryffel, F.; Houson, H.; Mohimani, H.; Kharbush, J. J.; Zeng, Y.; Vorholt, J. A.; Kurita, K. L.; Charusanti, P.; McPhail, K. L.; Nielsen, K. F.; Vuong, L.; Elfeki, M.; Traxler, M. F.; Engene, N.; Koyama, N.; Vining, O. B.; Baric, R.; Silva, R. R.; Mascuch, S. J.; Tomasi, S.; Jenkins, S.; Macherla, V.; Hoffman, T.; Agarwal, V.; Williams, P. G.; Dai, J.; Neupane, R.; Gurr, J.; Rodríguez, A. M. C.; Lamsa, A.; Zhang, C.; Dorrestein, K.; Duggan, B. M.; Almaliti, J.; Allard, P.-M.; Phapale, P.; Nothias, L.-F.; Alexandrov, T.; Litaudon, M.; Wolfender, J.-L.; Kyle, J. E.; Metz, T. O.; Peryea, T.; Nguyen, D.-T.; VanLeer, D.; Shinn, P.; Jadhav, A.; Müller, R.; Waters, K. M.; Shi, W.; Liu, X.; Zhang, L.; Knight, R.; Jensen, P. R.; Palsson, B. Ø.; Pogliano, K.; Linington, R. G.; Gutiérrez, M.; Lopes, N. P.; Gerwick, W. H.; Moore, B. S.; Dorrestein, P. C.; Bandeira, N. Sharing and Community Curation of Mass Spectrometry Data with Global Natural Products Social Molecular Networking. *Nat. Biotechnol.* **2016**, *34* (8), 828−837.

(17) Achenbach, H.; Mühlenfeld, A.; Weber, B.; Kohl, W.; Brillinger, G.-U. Stoffwechselprodukte von Mikroorganismen, XXVII[1] Cyclopaldsäure Und 3-O-Methyl-Cyclopolsäure, Zwei Antibiotisch Wirksame Substanzen Aus Aspergillus Duricaulis/Investigations on Metabolites of Microorganisms XXVII [1] Cyelopaldic Acid and 3-O-Methyl Cyclopolic Acid, Two Antibiotically Active Substances from Aspergillus duricaulis. *Zeitschrift für Naturforschung B* **1982**, *37* (8), 1091−1097.

(18) Tsantrizos, Y. S.; Ogilvie, K. K.; Watson, A. K. Phytotoxic Metabolites of Phomopsisconvolvulus, a Host-Specific Pathogen of Field Bindweed. *Can. J. Chem.* **1992**, *70* (8), 2276−2284.

(19) McMullin, D. R.; Tanney, J. B.; McDonald, K. P.; Miller, J. D. Phthalides Produced by Coccomyces Strobi (Rhytismataceae, Rhytismatales) Isolated from Needles of Pinus Strobus. *Phytochem. Lett.* **2019**, *29*, 17−24.

(20) Chen, H.-W.; Jiang, C.-X.; Li, J.; Li, N.; Zang, Y.; Wu, X.-Y.; Chen, W.-X.; Xiong, J.; Li, J.; Hu, J.-F. Beshanzoides A−D, Unprecedented Cycloheptanone-Containing Polyketides from Penicillium Commune P-4−1, an Endophytic Fungus of the Endangered Conifer Abies Beshanzuensis. *RSC Adv.* **2021**, *11* (63), 39781−39789.

(21) Hamberg, P.; Verweij, J.; Sleijfer, S. (Pre-)Clinical Pharmacology and Activity of Pazopanib, a Novel Multikinase Angiogenesis Inhibitor. *Oncologist* **2010**, *15* (6), 539−547.

(22) Cho, H.-D.; Moon, K.-D.; Park, K.-H.; Lee, Y.-S.; Seo, K.-I. Effects of Auriculasin on Vascular Endothelial Growth Factor (VEGF)-Induced Angiogenesis via Regulation of VEGF Receptor 2 Signaling Pathways in Vitro and in Vivo. *Food Chem. Toxicol.* **2018**, *121*, 612−621.

(23) Karar, J.; Maity, A. PI3K/AKT/MTOR Pathway in Angiogenesis. *Frontiers in Molecular Neuroscience* **2011**, DOI: 10.3389/fnmol.2011.00051.

(24) Tsuji-Tamura, K.; Sato, M.; Fujita, M.; Tamura, M. The Role of PI3K/Akt/MTOR Signaling in Dose-Dependent Biphasic Effects of Glycine on Vascular Development. *Biochem. Biophys. Res. Commun.* **2020**, *529* (3), 596−602.

(25) El Baba, N.; Farran, M.; Khalil, E. A.; Jaafar, L.; Fakhoury, I.; El-Sibai, M. The Role of Rho GTPases in VEGF Signaling in Cancer Cells. *Anal. Cell. Pathol.* **2020**, *2020*, 2097214.

(26) Guo, L. D.; Huang, G. R.; Wang, Y.; He, W. H.; Zheng, W. H.; Hyde, K. D. Molecular Identification of White Morphotype Strains of Endophytic Fungi from Pinus Tabulaeformis. *Mycological Research* **2003**, *107*, 680−688.

(27) GARDES, M.; BRUNS, T. D. ITS Primers with Enhanced Specificity for Basidiomycetes - Application to the Identification of Mycorrhizae and Rusts. *Mol. Ecol.* **1993**, *2* (2), 113−118.

(28) Vilgalys, R.; Hester, M. Rapid Genetic Identification and Mapping of Enzymatically Amplified Ribosomal DNA from Several Cryptococcus Species. *J. Bacteriol.* **1990**, *172* (8), 4238−4246.

(29) Yang, Y.; Bae, W. K.; Nam, S. J.; Jeong, M. H.; Zhou, R.; Park, S. Y.; Taş, I.; Hwang, Y. H.; Park, M. S.; Chung, I. J.; Kim, K. K.; Hur, J. S.; Kim, H. Acetonic Extracts of the Endolichenic Fungus EL002332 Isolated from Endocarpon Pusillum Exhibits Anticancer

https://doi.org/10.1021/acsomega.3c00876
ACS Omega 2023, 8, 12548−12557

Activity in Human Gastric Cancer Cells. *Phytomedicine* **2018**, *40*, 106−115.
(30) Nothias, L.-F.; Petras, D.; Schmid, R.; Dührkop, K.; Rainer, J.; Sarvepalli, A.; Protsyuk, I.; Ernst, M.; Tsugawa, H.; Fleischauer, M.; Aicheler, F.; Aksenov, A. A.; Alka, O.; Allard, P.-M.; Barsch, A.; Cachet, X.; Caraballo-Rodriguez, A. M.; Da Silva, R. R.; Dang, T.; Garg, N.; Gauglitz, J. M.; Gurevich, A.; Isaac, G.; Jarmusch, A. K.; Kameník, Z.; Kang, K. B.; Kessler, N.; Koester, I.; Korf, A.; Le Gouellec, A.; Ludwig, M.; Martin H., C.; McCall, L.-I.; McSayles, J.; Meyer, S. W.; Mohimani, H.; Morsy, M.; Moyne, O.; Neumann, S.; Neuweger, H.; Nguyen, N. H.; Nothias-Esposito, M.; Paolini, J.; Phelan, V. V.; Pluskal, T.; Quinn, R. A.; Rogers, S.; Shrestha, B.; Tripathi, A.; van der Hooft, J. J. J.; Vargas, F.; Weldon, K. C.; Witting, M.; Yang, H.; Zhang, Z.; Zubeil, F.; Kohlbacher, O.; Böcker, S.; Alexandrov, T.; Bandeira, N.; Wang, M.; Dorrestein, P. C. Feature-Based Molecular Networking in the GNPS Analysis Environment. *Nat. Methods* **2020**, *17* (9), 905−908.
(31) Tsugawa, H.; Cajka, T.; Kind, T.; Ma, Y.; Higgins, B.; Ikeda, K.; Kanazawa, M.; Vandergheynst, J.; Fiehn, O.; Arita, M. MS-DIAL: Data-Independent MS/MS Deconvolution for Comprehensive Metabolome Analysis. *Nat. Methods* **2015**, *12* (6), 523−526.
(32) *UCSD/CCMS - Spectrum Library*. https://gnps.ucsd.edu/ProteoSAFe/gnpslibraryspectrum.jsp?SpectrumID=CCMSLIB00010128698#%7B%7D (accessed 2023-02-28).
(33) *UCSD/CCMS - Spectrum Library*. https://gnps.ucsd.edu/ProteoSAFe/gnpslibraryspectrum.jsp?SpectrumID=CCMSLIB00010128671#%7B%7D (accessed 2023-02-28).
(34) *UCSD/CCMS - Spectrum Library*. https://gnps.ucsd.edu/ProteoSAFe/gnpslibraryspectrum.jsp?SpectrumID=CCMSLIB00010128697#%7B%7D (accessed 2023-02-28).
(35) Lee, K.; Kang, K. B.. *Raw NMR FID Data of Phthalides from the Endolichenic Arthrinium Sp. EL000127*, 2022; DOI: 10.5281/ZENODO.7375204.

https://doi.org/10.1021/acsomega.3c00876
ACS Omega 2023, 8, 12548−12557